# Machine learning for advanced solar cell production: adversarial denoising, sub-pixel alignment and the digital twin

**Matthias Demant*** **Leslie Kurumundayil** **Philipp Kunze** **Alexandra Woernhoer**

**Aditya Kovvali** **Stefan Rein**

Fraunhofer Institute for Solar Energy Systems, Freiburg, Germany
firstname.lastname@ise.fraunhofer.de

## Abstract

Photovoltaic is a main pillar to achieve the transition towards a renewable energy supply. In order to continue the tremendous cost decrease of the last decades, novel cell technologies and production processes are implemented into mass production to improve cell efficiency. Raising their full potential requires novel techniques of quality assurance and data analysis. We present three use-cases along the value chain where machine learning techniques are investigated for quality inspection and process optimization: Adversarial learning to denoise wafer images, alignment of surface structuring processes via sub-pixel coordinate regression, and the development of a digital twin for wafers and solar cells for material and process analysis.

## 1 Introduction

The transition to a renewable energy supply is a main driver to reduce carbon emission and slow down climate change. Photovoltaic (PV) is a key technology that already contributes to the mix of energy sources for a carbon-free energy production of the future. In order to win the competition against conventional energy sources, the costs of solar cell production must be further reduced to achieve grid parity even in countries with less favorable weather conditions.

Following the PV technology roadmap, novel production processes and characterisation methods are implemented to reduce costs and increase throughput and energy conversion efficiency. Smaller structures, higher measurements speeds and smarter processes challenge solar energy researchers. We introduce three use-cases along the PV value where novel machine learning techniques offer solutions and opportunities for equipment and solar cell manufacturers as shown in Figure 1. In all applications, we address real world problems and work with data which are experimentally created within our research pilot line.

During wafering the silicon ingot is sliced into thin wafers. The diamond wire sawing process was established as a cost efficient alternative to existing processes. Yet, implemented quality inspection methods fail to characterize the samples due to strong surface artifacts visible in the measurements. We investigate adversarial networks to denoise the images for quality inspection (Section 1.1).

*corresponding author

Tackling Climate Change with Machine Learning workshop at NeurIPS 2020.

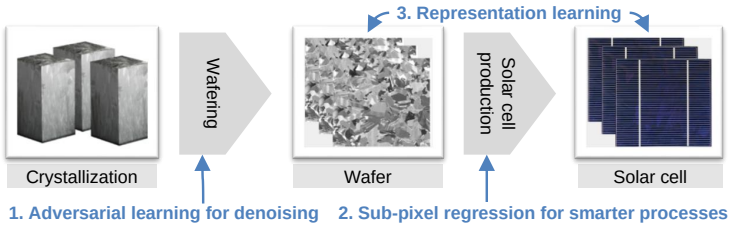


Figure 1: Use cases along the PV value chain

Our second application aims to increase the efficiency of solar cells through novel solar cell processes by developing aligned surface structuring and metallization processes. For calibration of camera and laser processes, a learning based method for coordinate regression is presented in Section 2.

Third, representation learning techniques are investigated for advanced wafer and solar cell analysis. We derive a digital twin of the solar cell which combines complex measurement data to a meaningful representation for material and process monitoring in Section 3.

### 1.1 Efficient wafering processes challenge material characterization

The diamond wire sawing (Bidiville et al. (2009)) process has been developed to replace slurry-based wafering. It has established as a standard process in industry due to its higher throughput, cost efficiency, environment-friendliness and smaller kerf loss. Although DWS is a novel wafering technology, it comes at the cost of surface damage to the silicon wafers. Current optical inspection tools are optimized to slurry-cut wafers which do not have strong macroscopic saw damage. The implemented algorithms fail to analyze images of DWS wafers due to the strong surface damage. In our first use case, machine learning techniques are investigated to remove artifacts from the noisy images.

**Adversarial networks for denoising.** Most machine learning techniques are based on supervised learning. In our case, paired data is not available since a wafer is either slurry-cut or diamond-cut. How can we train a network to remove the noise structures? A Generative Adversarial Network (GAN) (Goodfellow et al. (2014)) consists of a generator network and a discriminator network to give feedback about the quality of the result during training. In this work, an adversarial network called ResidualGAN, shown in Figure 2, is implemented for denoising the DWS wafer images. The generator G of the ResidualGAN is a combination of a U-Net (Ronneberger et al. (2015))

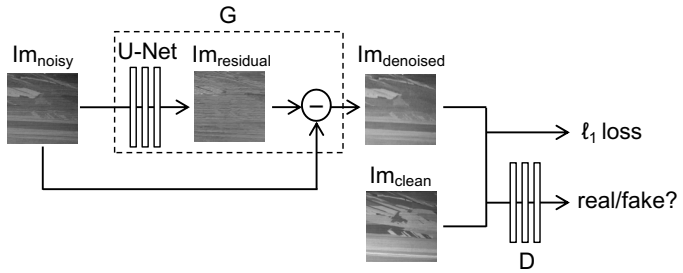


Figure 2: Schematic of a ResidualGAN

and a subtractor. A noisy image $Im_{noisy}$ is given as an input to the U-Net to extract the artifacts $Im_{residual}$. The subtractor removes this noise from the noisy wafer image to output the denoised image $Im_{denoised}$ which is classified as real or fake by the discriminator D to provide the generator a feedback. To train the adversarial network with an additional supervised loss, two different paired datasets, namely textured and synthetic data, are generated.

**Experimental datasets.** Datasets with optical images of noisy images, i.e. images of DWS wafers, and clean images, i.e. images of slurry-cut wafers, are created. First, a set of unpaired data was

selected from slurry-cut and DWS wafer images. Additionally, two datasets of paired images with and without noise were created for a supervised data analysis. For the second paired dataset, the DWS wafers go through an experimental process: Images of the DWS wafers are captured before and after a wet-chemical texturing process, which removes the surface damage and thus the noise. Our third (paired) dataset contains synthetic data. Here, the saw marks on the DWS wafers are analyzed in detail and replicated onto the slurry-cut wafer images to create a synthetic dataset of clean and noisy images.

**Experimental results.** The ResidualGAN is trained on unpaired data of DWS and slurry-cut images but fails to converge due to mode collapse. Mode collapse occurs when the generator learns how to generate samples from a few modes of the data distribution but misses many other modes, even though samples from the missing modes occur throughout the training data (Srivastava et al. (2017)). In addition, a supervised loss is considered by using the textured dataset, as well as the synthetic dataset. An example of the results is shown in Figure 3. The first column shows the noisy input image that is to be denoised. The second image shows the output of the ResidualGAN trained on unpaired data. The model produced an unrealistic slurry-cut image which does not correlate to the input image. The third and fourth columns show the results obtained by the ResidualGAN with the textured data and the synthetic data, respectively. In case of the textured training data, the noise structures have been removed from most of the wafer leaving the grain boundaries slightly blurred in some areas. For the synthetic training data, the saw marks have not been removed completely, but the image shows nevertheless sharp grain boundaries.

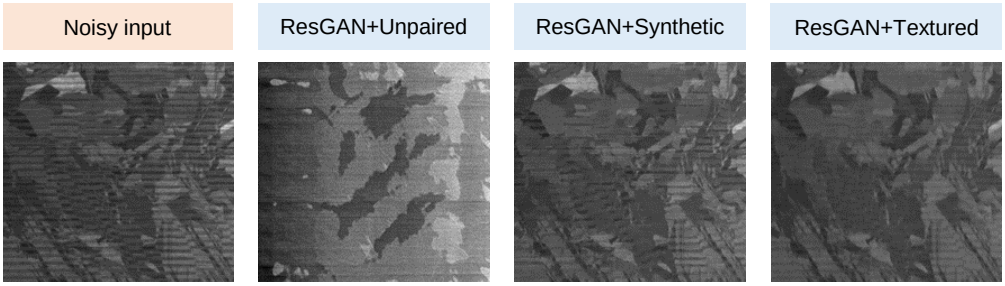


Figure 3: DWS wafer image as noisy input image (left) and denoised images of ResidualGAN (middle left) trained on unpaired data, (middle right) synthetic data and textured data (right)

## 2 Smart production

### 2.1 Need and challenge of process alignment

Technology developments along the road-map for industrial solar cell production require the alignment of surface structuring processes (Werner et al. (2017)). The implementation of a selective emitter process using laser doping, for example, requires the adaptation of the laser structure to the pattern of a subsequent screen printing process. An increase in solar cell efficiency up to $0.3\%_{abs}$ is expected by selectively increasing the doping concentration below the metal contact. On the one hand, contact formation can be improved through lower series resistance losses. On the other hand, the localized process allows a lower doping concentration at the non-metallized surfaces and thus improved recombination properties.

A precise alignment procedure has to be established within an inline measurement systems to adjust the positions of the laser openings to the printed pattern. The alignment has to consider deviations in both processes: the screen deforms continuously during cell production. Also the quality of a conventional laser calibration as well as the inline measurement system are not sufficient for increasingly narrow contact structures. For most inline measurement systems in PV production, the sample is moving on a conveyor belt beneath a line scanning camera. A solid calibration sample will not bend like a wafer and vary in sample thickness.

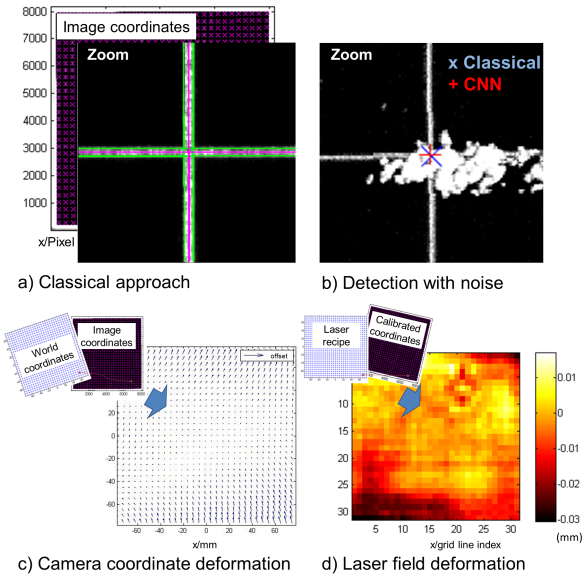


Figure 4: Coordinate detection (a) with classical methods and (b) deep neural networks for noisy images for (c) camera and (d) laser calibration

### 2.2 Camera and laser calibration

We introduce a calibration procedure for an inline camera system as well as a laser field correction based on a laser inscribed calibration sample. The sub-pixel accurate coordinates of the calibration pattern are detected via different computer vision techniques within the images.

**Classical approach.** Using classical image processing techniques, the edge of the laser structure is identified at both sides of the opening for horizontal and vertical line structures as shown by the green lines in Figure 4 a. The intersection of a horizontal and a vertical averaged center line indicates the intersection coordinate. The results appear very precise, but suffer from noise in the images.

**Sub-pixel regression.** A CNN is trained for sub-pixel accurate coordinate regression to avoid detection errors due to noise and allow for a fast image analysis. We combine a dense neural network (He et al. (2015)) as backbone with the differentiable spatial to numerical transform (DSNT) (Huang et al. (2016)). The network is trained with the coordinates gained from classical image processing. Intensive data augmentation by adding realistic noise structures increased the robustness of the detections as shown in Figure 4 b. The coordinate with noise deviates only by 1.6 pixels from the classical results evaluated without noise.

**Calibration.** The camera calibration was performed based on microscopic reference data. A Procrustes transformation (Gower (1975)) is applied to match the real world data to the inline acquired data. The calibration pattern is given by fitting polynomials to the remaining deformation (Figure 4 c). The deformation pattern of the inline system varies strongly to classical camera distortions. For calibration, the images are warped according to the deformation pattern.

For the laser calibration, the image coordinates are identified after camera calibration and compared to the laser recipe. Again a Procrustes transformation is applied to overcome a varying position of the sample in the image. The laser deformation pattern is shown in Figure 4 d.

Finally, the deformation of the printed grid structure is analyzed with the calibrated camera system and the laser recipe is updated accordingly. Figure 5 shows the successful alignment of the two processes which has been accomplished within our experiment.

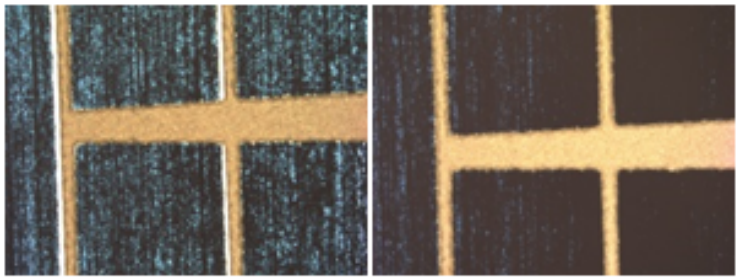

Figure 5: (Left) Laser openings (white) and printed structures (gold) without calibration. (Right) After calibration the laser openings are occluded.

## 3 Representation learning for wafer and solar cell analysis

Quality inspection using spatially resolved inline measurement data opens up new process control options for PV production. Optical and electrical measurements reveal material and production related defects, e.g., material defects, broken grid contacts or shunts. Image evaluation methods available on the market are based on engineered features or models trained with human labeled data, which, however, can only capture a fraction of the available information in view of the complex relationships in the data. We use representation learning techniques to derive a compact and yet meaningful representation of the solar cell from the measured data. Our digital twin learns the essential quality information on the basis of empirical data.

**Material quality prediction.** For this purpose, measurements are combined via deep learning to predict physical quality parameters. In previous works (Demant et al. (2018a)), this approach was presented for material analysis at wafer level. A prediction of the solar cell quality was performed via a multivariate densely connected regression model. The model learns to predict the open-circuit voltage of PERC solar cells (Green (2015)) based on photoluminescence images (Trupke et al. (2006)). The high prediction quality is shown in Figure 6.

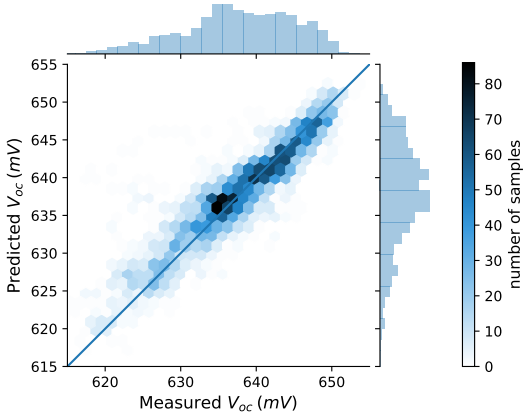


Figure 6: Measured and predicted $V_{oc}$ values from PL-images of as-cut wafers for multicrystalline wafers.

**Solar cell monitoring.** A monitoring of cell production can be drawn from optical, electrical and thermography measurements of solar cells. The prediction of the current-voltage parameters from the images is used for the creation of a digital twin of the sample. The model learns a meaningful description of the state of the solar cell by creating a compact representation from high-dimensional measurement images, which enables a successful quality prediction. A look into the model shows the activation of the neurons. On the one hand, activation maps reflect the expected spatially resolved quality distribution from the network's point of view (Zhou et al. (2016)). The neural activation

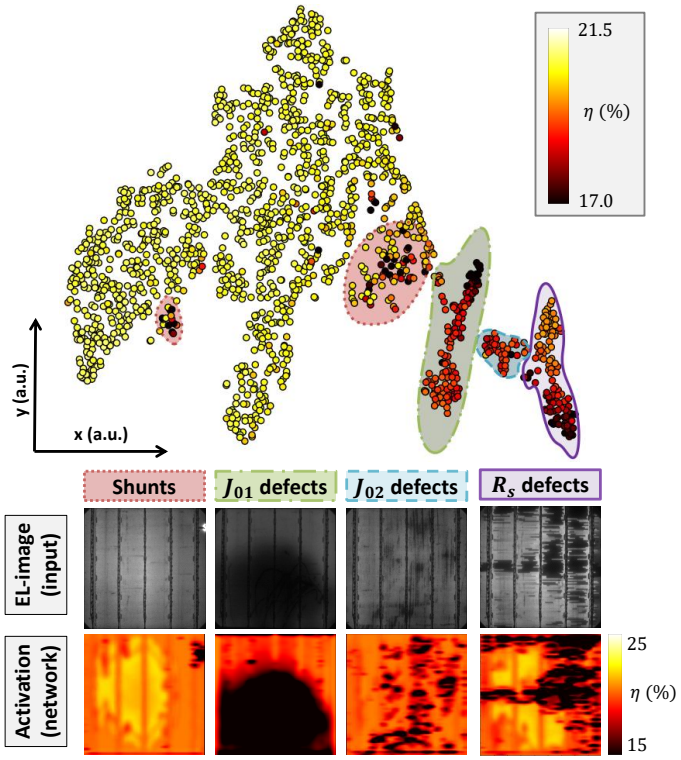


Figure 7: Visualization of the representations derived from the network activation. (Top) All samples are visualized in a 2D embedding and colored according to their cell efficiency. Four different defect clusters are identified within the oval areas corresponding to the solar cell defects. (Bottom) Exemplary EL-image and activation map for each defect.

can be scaled to physical units (Demant et al. (2018b)), thus, showing the samples distributions of efficiency or open-circuit voltage. The quality maps allow to draw conclusions about the cause and effect of defects. On the other hand, the representation also causes an efficient storage of the data and their comparability for fast defect classification.

**Experimental.** The model learns how to derive a digital twin from a data set of 1600 cells by means of Electroluminescence (EL)-images (Fuyuki et al. (2005)). For analysis, the representations of the solar cells are viewed in a 2-D plot. Applying the t-SNE technique (van der Maaten & Hinton (2008)), the illustration has been simplified in such a way that neighboring points are similar in their representation: Groups of solar cells are formed which have specific defects highlighted by a colored background. A typical EL-image is shown for each defect group. Also the quality map with the spatially resolved efficiency is shown, which is lower in regions with many defects. The described technique can be used to classify cells automatically in order to sort out samples of certain representations or defect groups.

## 4 Conclusion

In this study, novel machine learning techniques are applied in three different use cases for photovoltaic production. First, GANs are successful at denoising DWS wafer images which allows quality inspection despite strong surface damage. Second, advanced structured solar cell designs were produced which require aligned surface structuring processes. By means of sub-pixel accurate coordinate regression camera and laser systems were calibrated with high precision and robustness. This lead to a perfect overlap of both structuring process and an increase in solar cell efficiency. Third, we showed the potential of representation learning for a automatic process monitoring based on the meaningful compression of multiple image sources within a CNN for current-voltage prediction.

## References


Bidiville, A., Wasmer, K., Kraft, R., and Ballif, C. Diamond wire-sawn silicon wafers - from the lab to the cell production. 2009.

Demant, M., Virtue, P., Kovvali, A., Yu, S. X., and Rein, S. Learning quality rating of multicrystalline si-wafers via convolutional regression networks. *IEEE, Journal of Photovoltaics*, 9(4):1064–1072, 2018a.

Demant, M., Virtue, P., Kovvali, A., Yu, S. X., and Rein, S. Visualizing material quality and similarity of mc-si wafers learned by convolutional regression networks. *IEEE, Journal of Photovoltaics*, 9 (4):1073 – 1080, 2018b.

Fuyuki, T., Kondo, H., Yamazaki, T., Takahashi, Y., and Uraoka, Y. Photographic surveying of minority carrier diffusion length in polycrystalline silicon solar cells by electroluminescence. *Applied Physics Letters*, 86(26):262108, 2005.

Goodfellow, I. J., Pouget-Abadie, J., Mirza, M., Xu, B., Warde-Farley, D., Ozair, S., Courville, A. C., and Bengio, Y. Generative adversarial nets. In *Advances in Neural Information Processing Systems 27: Annual Conference on Neural Information Processing Systems 2014, December 8-13 2014, Montreal, Quebec, Canada*, pp. 2672–2680, 2014.

Gower, J. C. Generalized procrustes analysis. *Psychometrika*, 40(1):33–51, 1975.

Green, M. A. The passivated emitter and rear cell (perc): From conception to mass production. *Solar Energy Materials and Solar Cells*, 143(Supplement C):190 – 197, 2015. ISSN 0927-0248. doi: https://doi.org/10.1016/j.solmat.2015.06.055.

He, K., Zhang, X., Ren, S., and Sun, J. Deep residual learning for image recognition. *CoRR*, abs/1512.03385, 2015. URL `http://arxiv.org/abs/1512.03385`.

Huang, G., Liu, Z., and Weinberger, K. Q. Densely connected convolutional networks. *CoRR*, abs/1608.06993, 2016. URL `http://arxiv.org/abs/1608.06993`.

Ronneberger, O., Fischer, P., and Brox, T. U-net: Convolutional networks for biomedical image segmentation, 2015.

Srivastava, A., Valkov, L., Russell, C., Gutmann, M. U., and Sutton, C. Veegan: Reducing mode collapse in gans using implicit variational learning, 2017.

Trupke, T., Bardos, R., Schubert, M., and Warta, W. Photoluminescence imaging of silicon wafers. *Applied Physics Letters*, 89(4):044107, 2006.

van der Maaten, L. and Hinton, G. E. Visualizing high-dimensional data using t-sne. *Journal of Machine Learning Research*, 9:2579–2605, 2008.

Werner, S., Lohmüller, E., Saint-Cast, P., Greulich, J., Weber, J., Schmidt, S., Moldovan, A., Brand, A., Mack, S., et al. Key aspects for fabrication of p-type cz-si perc solar cells exceeding 22% conversion efficiency. 2017.

Zhou, B., Khosla, A., A., L., Oliva, A., and Torralba, A. Learning Deep Features for Discriminative Localization. *CVPR*, 2016.